Transient Receptor Potential Canonical 3 (TRPC3) Channels Are Required for Hypothalamic Glucose Detection and Energy Homeostasis

Chloé Chrétien, Claire Fenech, Fabienne Liénard, Sylvie Grall, Charlène Chevalier, Sylvie Chaudy, Xavier Brenachot, Raymond Berges, Katie Louche, Romana Stark, et al.

Transient Receptor Potential Canonical 3 (TRPC3) channels are required for hypothalamic glucose detection and energy homeostasis

Running title: TRPC3: a new actor in hypothalamic glucose detection

Chloé Chrétien[1], Claire Fenech[1], Fabienne Liénard[1], Sylvie Grall[1], Charlène Chevalier[1], Sylvie Chaudy[1], Xavier Brenachot[1], Raymond Berges[1], Katie Louche[2], Romana Stark[3], Emmanuelle Nédélec[1], Amélie Laderrière[1], Zane B. Andrews[3], Alexandre Benani[1], Veit Flockerzi[4], Jean Gascuel[1], Jana Hartmann[5], Cédric Moro[2], Lutz Birnbaumer[6], Corinne Leloup[1], Luc Pénicaud[1], Xavier Fioramonti[1,$].

[1]Centre des Sciences du Goût et de l'Alimentation, CNRS, INRA, Univ. Bourgogne Franche-Comté, F-21000 Dijon, France.
[2]INSERM UMR1048, University of Toulouse, Institute of Metabolic and Cardiovascular Diseases, Obesity Research Laboratory, Toulouse, France.
[3]Biomedicine Discovery Institute, Metabolic Disease and Obesity Program, Department of Physiology, Monash University, Clayton, Victoria 3196, Australia.
[4]Experimental and clinical Pharmacology and Toxicology, Saarland University School of Medicine, Homburg, Germany.
[5]Institute of Neuroscience and Center for Integrated Protein Science, Technical University Munich, 80802 Munich, Germany.
[6]Neurobiology Laboratory, National Institute of Environmental Health Sciences, Research Triangle Park, NC 27709, USA; and Institute of Biomedical Research (BIOMED), Catholic University of Argentina, C1107AFF, Argentina.

Word count: 4587

[$]To whom correspondence should be addressed: Xavier Fioramonti, Centre des Sciences du Goût et de l'Alimentation, 9[E] Boulevard Jeanne d'Arc, 21000 Dijon, France. Tel.: +33-3-80-68-16-43; Fax: +33-3-80-68-16-01; E-mail: xavier.fioramonti@dijon.inra.fr

Diabetes Publish Ahead of Print, published online November 29, 2016

ABSTRACT

The medio-basal hypothalamus (MBH) contains neurons capable of directly detecting metabolic signals such as glucose to control energy homeostasis. Among them, glucose-excited (GE) neurons increase their electrical activity when glucose rises. In view of previous work, we hypothesized that Transient Receptor Potential Canonical type-3 (TRPC3) channels are involved in hypothalamic glucose detection and the control of energy homeostasis.

To investigate the role of TRPC3, we used constitutive and conditional TRPC3-deficient mice models. Hypothalamic glucose detection was studied *in vivo* by measuring food intake and insulin secretion in response to increased brain glucose level. The role of TRPC3 in GE neuron response to glucose was studied using *in vitro* calcium imaging on freshly dissociated MBH neurons.

We found that whole body and MBH TRPC3-deficient mice have increased body weight and food intake. The anorectic effect of intracerebroventricular glucose and the insulin secretory response to intracarotid glucose injection are blunted in TRPC3-deficient mice. TRPC3 loss-of-function or pharmacological inhibition blunts calcium responses to glucose in MBH neurons in vitro.

Together, our results demonstrate that TRPC3 channels are required for the response to glucose of MBH GE neurons and central effect of glucose on insulin secretion and food intake.

ABBREVIATIONS:

ARC: arcuate nucleus; **EWAT:** epididymal white adipose tissue; **FFA:** free fatty acids; **GE neurons:** glucose-excited neurons; **GI neurons:** glucose-inhibited neurons; **ICV:** intracerebroventricular; **IPGTT:** intraperitoneal glucose tolerance test; **ITT:** insulin tolerance test; **MBH:** mediobasal hypothalamus; **NSCC:** non-selective cation conductance; **OAG:** O-acyl-glycerol; **PLC:** phospholipase C; **Pyr3:** pyrazole 3; **ROS:** reactive oxygen species; **TRPC:** transient receptor potential canonical; **VMN:** ventromedial nucleus

INTRODUCTION

The brain and more particularly the hypothalamus play a critical role in the control of energy homeostasis by regulating feeding behavior and the activity of peripheral organs through humoral and neural systems. Within the medio-basal hypothalamus (MBH, including the arcuate (ARC) and ventromedial nuclei (VMN)), this control relies on neurons able to directly detect metabolic signals such as hormones (e.g. leptin, insulin and ghrelin) and nutrients (e.g. glucose, fatty and amino acids) (1). Among them, specialized glucose-sensing neurons adapt their electrical activity in response to changes in glucose levels. Glucose-excited (GE) neurons increase, whereas glucose-inhibited (GI) neurons decrease, their electrical activity when extracellular glucose rises (2-5). The properties of these neurons allow the brain to detect increased blood glucose level which in turn triggers appropriate responses including enhanced insulin secretion, reduced food intake and hepatic glucose production (6-8).

Identifying the signaling pathway(s) involved in glucose-sensing neurons has aroused the scientific community for half a century. Our group and others showed that mitochondrial reactive oxygen species (ROS) are produced in the MBH in response to increased brain glucose levels and are involved in the regulation of food intake and insulin secretion (7-10). In addition, based on the key role of ion channels in controlling neuronal excitability, several groups have focused on identifying channels responsible for nutrient or hormone sensing. This effort has highlighted ATP-dependent potassium (K_{ATP}) channels as key players in neuronal glucose-sensing (see for review (11)). However, even if the role of K_{ATP} is undeniable, we and others have pointed out that additional channels might be critical for glucose sensing (11-13). More specifically, we found that the opening of channels exhibiting a non-selective cation conductance (NSCC channels) is involved in the glucose response of a sub-population of GE neurons in the MBH (12).

Transient receptor potential (TRP) and particularly TRP canonical (TRPC) channels represent one of the largest family of NSCC channels (14). A link between TRPC channels and the control of energy metabolism has been proposed based on studies showing that TRPC channels mediate some of the effects of leptin and insulin on hypothalamic neuronal activity (15-17). Nevertheless, the role of TRPC channels in hypothalamic glucose detection and central control of energy homeostasis remains unknown. Interestingly, TRPC3 channels activity is regulated by ROS suggesting that these channels may be involved in glucose sensing in GE neurons of the MBH (18; 19). Therefore, the overall goal of the present study was to determine whether TRPC3 channels are part of the glucose-sensing machinery in GE neurons of the MBH and to assess their contribution in central glucose effects.

MATERIAL AND METHODS

Animals: Male outbred Sprague-Dawley rats or inbred C57BL/6J mice were purchased from Charles River France. TRPC3 deficient (TRPC3 KO) mice, control wild type (TRPC3 WT, same genetic background) and TRPC3$^{lox/lox}$ (exon 7 of Trpc3 is flanked by LoxP sites) mice were provided by the Comparative Medicine Branch of the National Institute of Environmental Health Sciences (The Research Triangle Park, Durham, NC) (20). Animals were housed in a controlled environment (12 h light/dark cycle, light on at 7:00 am) with food and water available *ad libitum*. All procedures were performed in agreement with the European Directive 2010/63/UE and approved by French Ministry of Research and the local ethic committee of the University of Burgundy (C2EA Grand Campus Dijon N° 105; agreement N° 02404.02).

RT-PCR: Following extraction (RNAEasy, Qiagen) mRNA quality/quantity was assessed by microelecrophoresis (Experion, Biorad). Reverse transcription (Quantitect RT, Qiagen) was performed on standardized amounts of starting RNA for all samples in each study. qPCR was carried out on a SteponePlus thermocycler (Applied Biosystems) using either SYBR green (FastSYBR master mix, Applied Biosystems) or hydrolysis probes (Taqman Assay, Gene Expression master mix, Applied Biosystems) on standardized cDNA (starting RNA equivalent 40-70ng). Sequence or reference of primers for SYBR green and Taqman assays are presented in Supp. Table 1.

Western blots: Lysates were prepared by homogenising brain in RIPA buffer containing proteases inhibitors using a Tissue Lyser (Qiagen). Lysates were diluted in Laemmli buffer and samples (200 µg of protein) were loaded onto a 4-15% TGX precast gel (Biorad). Gel was fast transferred onto PVDF membrane using Biorad's Transblot Turbo. Membranes were blocked in 3% blocking reagent (BioRad) then incubated with a homemade rabbit

anti-TRPC3 (1:100 - overnight at 4°C, (21)). Secondary immunodetection was carried out with anti-rabbit IgG-HRP (1:50000 – 1h at room temperature) and the chemiluminescent signal was acquired on a Chemidoc station (Biorad). The specificity of the antibody was confirmed using TRPC3 KO as presented in Supp. Figure 1.

Virus injection: TRPC3$^{lox/lox}$ mice (8-10 week old, in which exon 7 of Trpc3 is flanked by LoxP sites; (20)) were anaesthetised with isoflurane and placed on a stereotaxic apparatus (Kopf instrument). Adeno-associated virus expressing Cre and GFP (AAV-Cre/GFP) or GFP (AAV-GFP) under the CMV (AAV-Cre/GFP) or CBA (AAV-GFP) promoter were injected bilaterally into the MBH (stereotaxic coordinates relative to bregma: -1.4 mm antero-posterior, +0.4 mm lateral and -5.6 mm dorso-ventral from the dura at a rate of 50 nl/min for 5 min per side. The plasmid CBA.nls-myc-Cre/eGFP expressing the myc-nls-Cre-GFP fusion protein (22). AAV-Cre/GFP or AAV-GFP serotype 2/9 (6×10^{11} genomes/ml) were produced by the viral production facility of the UMR INSERM 1089 (Nantes, France).

Glucose (IPGTT) and insulin (ITT) tolerance tests: Glucose and insulin tolerance tests were performed in 5h-fasted mice by measuring blood glucose (Roche Accu-Check) from the tail vein after oral glucose (2 g/kg) or intraperitoneal (IP) insulin (0.3 U/kg) administration. Blood samples were collected for insulin measurements during the OGTT using a bead-based alphaLISA insulin immunoassay kit (Perkin Elmer).

Central glucose-induced insulin secretion: As previously described (23), a silastic catheter was implanted into the left carotid artery in the cranial direction in anesthetized mice or rats (pentobarbital, 60 mg/kg) and secured in place with sutures. Despite its potential role on autonomic output, we use pentobarbital because it is, to our knowledge,

the only approved anesthetic not impacting blood glucose level (24; 25). Fifteen minutes after the surgery, a bolus of glucose (mice: 25 mg/kg in 30 µl over 30 seconds; rats: 9 mg/kg in 100 µl over 60 seconds; osmolarity adjusted to 300-310 mOsM with NaCl) was administered through the catheter. Blood samples were collected from the tail vein to measure blood glucose and plasma insulin levels.

Food intake: Food intake was measured by hand or using the BioDaq food intake measuring system (Research Diets) in singly housed animals. Three measurements of 24h food intake were average per mice over a week.

Fasting-Refeeding tests in response to increased brain or IP glucose level: Prior to brain glucose injection, animals (8-10 week old) were anaesthetised with isoflurane and placed on a stereotaxic apparatus (Kopf instrument) to implant a guide cannula (Plastics One) into the right lateral ventricle (stereotaxic coordinates relative to bregma: -0.5 mm antero-posterior, +1 mm lateral and -2.1 mm dorso-ventral from the dura). Seven days after the surgery, naïve or canulated animals were food deprived for 18h with *ad libitum* access to water. Glucose was administered through the guide cannula (125 µg in 2 µl at a rate of 0.4 µl/min; sucrose was used as control to control osmolarity effects) or IP (2 g/kg; NaCl 0.9 % was used as control) 1h before the onset of the dark cycle. Access to food was restored 30 minutes after intracerebroventricular (icv) injection and food intake was measured during 6 hours.

Calcium imaging on primary culture of dissociated MBH neurons: Dissociated MBH neurons were prepared from brain of 4/5-weeks-old TRPC3 WT or KO mice or rats as described previously (26-28). Briefly, MBH explants were dissected from 250 µm brain slices cut with a vibroslice (Leica). MBH cells were mechanically dissociated with papain

using the “neural tissue Dissociator Kit” (MACS Miltenyi Biotec), plated on poly-L-lysine (50 µg/ml)-coated glass coverslips in astrocyte-conditioned media overnight prior to calcium imaging experiments. Astrocyte-conditioned media was prepared as previously described (29) from MBH astrocytes plated on poly-L-lysine (50 µg/ml)-coated dishes and maintained in Neurobasal-A media (Invitrogen) containing (in mM) 2.5 D-glucose, 1 L-lactate, 0.23 L-pyruvate, 10% FBS, 0.5 L-glutamine, 100 U/ml penicillin/streptomycin and 10 µg/ml gentamycin, supplemented with 1 % B-27 (Invitrogen).

MBH neurons were loaded for 20 min with 0.5 µM Fura-2/acetoxymethyl ester (Fura-2/AM; Molecular Probes) in Hepes buffer balanced salt solution (HBSS) containing 2.5 mM of D-glucose supplemented with 0.002% pluronic acid. After the incubation, cells were mounted in a thermostatically regulated microscope chamber (37°C) mounted on an inverted microscope (Olympus IX 70). Fura-2 fluorescence images, acquired each 10 seconds by alternating excitation at 340 and 380 nm and emissions (420–600 nm), were collected using a cooled, charge-coupled device (CCD) camera with the Live Aquisition software (TiLL Photonics). Values for the 340/380 nm fluorescence ratio, representative of $[Ca^{2+}]_i$, were obtained after correction for background fluorescence values.

Glucose-excited (GE) neurons were identified in response to 2.5 to 10 mM increase in glucose level. 10 mM is higher than levels of glucose found brain areas including the hypothalamus (see for review (30)). Nevertheless, in view of the presence of fenestrated capillaries in the ventral part of the ARC (31), we could speculate that glucose level can locally be closer to blood level and rises above 5 mM. Changes in $[Ca^{2+}]_i$ were quantitated by calculating the integrated area under the curve (AUC) of each glucose response with the TiLL Photonics software. Neurons were considered as GE if the increase in $[Ca^{2+}]_i$ in response to 2.5-10 mM increased glucose level occurred between 2 and 20 minutes of treatment, had an amplitude > 0.1 (ratio 340/380), last at least 30 seconds and was transient. At the end of each recording, neuronal excitability was verified by measuring

Ca^{2+} response to 50 mM KCl. Neurons showing no response to KCl were not taken into consideration for analysis. We verified that the overall excitability of MBH GE neurons (amplitude of the calcium response to KCl) was not affected by any TRPC or K_{ATP} modulators or antioxidants, as well as in neurons isolated from TRPC3 KO mice (data not shown). Analysis of each experiment was obtained from at least 3 independent cultures prepared from at least 6 animals.

Expression of data and statistics: Data are expressed as means ± SEM. Intergroup comparisons were performed by ANOVA with Bonferroni post hoc tests or Student's *t*-test as described in figure legends using GraphPad Prism 5 software. $p < 0.05$ was set as significant.

RESULTS

TRPC3 channels are expressed in the MBH. The first aim of the study was to determine whether TRPC3 channels are expressed in the MBH where GE neurons are located. TRPC3 channels are known to be expressed in several peripheral tissues including muscles, liver and white adipose tissue (32). Within the brain, high TRPC3 expression has been reported in the cerebellum and cortex (33). In the hypothalamus, expression of TRPC3 channels has been detected but not investigated in specific nuclei (33). We found using qPCR and western blots (see online supplementary method) that TRPC3 channels are expressed in the MBH (Figure 1) as well as in other brain regions and peripheral tissues.

MBH TRPC3 channels are critical for the regulation of body weight and food intake. The role of TRPC3 channels in the control of energy homeostasis was investigated using whole body TRPC3-deficient (TRPC3 KO) mice. TRPC3 KO mice have impaired motor coordination but the impact of TRPC3 deficiency on the metabolic status has never been investigated (20). We found that TRPC3 KO mice have increased body weight associated with increased nocturnal food intake (Figure 2A, B). Change in food intake is not associated with changes in the expression level of MBH neuropeptides regulating food intake (Figure 2C). In addition, TRPC3 KO mice show an increased fasting blood glucose level associated with mild glucose intolerance (Figure 2D, E). However, the mild glucose intolerance in TRPC3 KO mice is not associated with alteration of insulin levels during the IPGTT (Supp. Figure 2A) or with insulin sensitivity (Supp. Figure 2B, C). The decrease in blood glucose level during an ITT (Supp. Figure 2B) or the quantification of phosphorylation level of the protein AKT (P-AKT, marker of insulin signaling) in skeletal muscle, epididymal white adipose tissue (EWAT) or liver (Supp. Figure 2C, (34)) are not statistically different between TRPC3 KO and WT mice. These data suggest that TRPC3

channels are involved in the control of food intake, body weight and glucose homeostasis which is in agreement with TRPC3 expression in metabolically active tissue and organs (32).

To investigate the role of TRPC3 channels expressed in the MBH in the control of energy and glucose homeostasis, we selectively invalidated TRPC3 expression in this area using Cre expressing AAV injected in the MBH of TRPC3$^{lox/lox}$ mice (referred as TRPC3^{MBH} KO mice, Figure 3A). TRPC3 gene expression is significantly reduced in the MBH of TRPC3^{MBH} KO mice as compared to controls (Figure 3B). TRPC3^{MBH} KO mice show an increased body weight gain 6 weeks following AAV injection, associated with an increased food intake during the sixth week (Figure 3C, D). The increased body weight gain is significantly correlated with the reduction of TRPC3 expression (Pearson r = -0.71, p = 0.01; Supp. Figure 3). Change in body weight gain in TRPC3^{MBH} KO mice is however not associated with changes in fasting blood glucose level or glucose tolerance (Figure 3E, F). Together, these data show that MBH TRPC3 channels are critical for food intake and body weight control but do not seem to directly regulate glucose homeostasis.

Central TRPC3 channels are required for central glucose detection. We then tested whether MBH TRPC3 channels are involved in brain glucose detection. To this end, we measured food intake and insulin secretion in response to increased brain glucose level in TRPC3 KO mice. As previously reported (35), ICV injection of glucose decreases food consumption in WT mice (Figure 4A). The anorectic effect of central glucose is totally blunted in TRPC3 KO mice (Figure 4A). Similarly, the effect of glucose on food intake in response to an IP injection of glucose is blunted in TRPC3 KO mice (Figure 4B). Importantly, the anorectic effect of IP glucose injection is also reduced in the TRPC3^{MBH} KO mice (Supp. Figure 4).

As previously described, the delivery of a glucose bolus to the brain via an intra-carotid injection that does not change peripheral blood glucose triggers a rapid and transient increase in plasma insulin via activation of the hypothalamic-pancreatic axis (23; 36). Our data show that insulin secretion induced by intra-carotid glucose administration is blunted in TRPC3 KO mice compared to WT controls (Figure 4C).

To further highlight the importance TRPC3 channels in MBH glucose detection, we selectively inhibited their activity by injecting the TRPC3 inhibitor pyrazole-3 (Pyr3) into the MBH of rats before the intra-carotid glucose bolus (Figure 4D). Our results show that Pyr3 inhibits intra-carotid glucose-induced insulin secretion (Figure 4D). Together, our findings demonstrate that MBH TRPC3 channels are required for brain glucose detection and the associated regulation of food intake and insulin secretion.

TRPC3 channels participate in the response of MBH GE neurons to glucose. We performed wide-field single cell imaging of $[Ca^{2+}]_i$ using the Fura-2 calcium probe in freshly dissociated MBH cells to study their direct response to glucose, as described previously (26; 27; 37; 38). Using this approach, we found that ~9 % of MBH neurons tested were identified as GE neurons as they harbor a transient increase in $[Ca^{2+}]_i$ in response to a raise in glucose level from 2.5 to 10 mM (Supp. Figure 5). Interestingly, the responses of MBH GE to two consecutive 2.5-10 mM increase in glucose level are similar in term of magnitude (Supp. Figure 5B, C). The glucose response latency is however shorter for the second increase in glucose level (Supp. Figure 5D).

To determine the role of TRPC3 channels in the response to glucose of MBH GE neurons, we first studied these neurons in dissociated MBH cells from TRPC3 KO or WT mice. The number of MBH GE neurons recorded did not differ in TRPC3 KO vs. WT mice (TRPC3 WT: 6.1 ± 0.5% *vs.* KO: 5.9 ± 0.4 %; $p>0.05$). However, the glucose response magnitude

is significantly decreased in TRPC3 KO mice (Figure 5A-C). The latency of GE neurons to respond to glucose is also significantly increased in MBH cells from TRPC3 KO mice (Figure 5D). These data suggest TRPC3 channels regulate the responsiveness of MBH GE neurons.

We confirmed these data using a pharmacological approach in dissociated cells isolated from rat MBH. Our results show that the non-selective TRPC channel inhibitor SKF96365 (39) strongly inhibits glucose responses in all GE neurons tested (n = 27/27 GE neurons tested) (Figure 6A, D). SKF96365 also significantly increases the latency of the glucose response of GE neurons (Figure 6E). Moreover, the TRPC3 channel inhibitor Pyr3 (39), reduced the response to glucose in ~70% of GE neurons (n = 26/37 GE neurons tested) (Figure 6B, D). Interestingly, the TRPC3 activator Oleoyl-acyl-glycerol (OAG, (40)) mimics glucose response, without any change in glucose levels, in ~70% of GE neurons (n=13/20 GE neurons tested) (Figure 6C, D). The latency of the glucose response of GE neurons is not affected by Pyr3 or OAG (Figure 6E). Together, these data show that TRPC3 is a key component of the glucose-sensing machinery in MBH GE neurons.

ROS but not K_{ATP} channels are necessary for the response to increased glucose level by MBH glucose-excited (GE) neurons. We and others previously showed that a sub-population of MBH GE neurons increase their electrical activity in response to increased glucose level through the opening of a NSCC rather than using a K_{ATP}-dependent pathway (12; 13). We confirm these data by showing that the K_{ATP} channel opener diazoxide does not significantly inhibit the magnitude of glucose response in MBH GE neurons (Supp. Figure 6).

As our group demonstrated that MBH ROS production is important for brain glucose detection and the regulation of food intake and insulin secretion (7; 8), we tested whether ROS mediate the response of MBH GE neurons to increased glucose. Our results show

that responses to glucose in ~95% of GE neurons are robustly blocked by a cocktail of antioxidants trolox/glutathione (n=26/27 GE neurons tested) or the H_2O_2-decomposing enzyme catalase (n=13/14 GE neurons tested; Figure 7A-C). Antioxidants do not alter the latency of the glucose response of GE neurons (Figure 7D). Altogether, these data demonstrate that ROS, particularly H_2O_2, but not K_{ATP} channels are necessary for the detection of increased glucose levels by MBH GE neurons.

DISCUSSION

Detection of changes in glucose level is dependent on several key processes including transport, metabolism and membrane excitability, which is unique to glucose and different from neurotransmitter/hormones. Several components of the glucose-sensing machinery have already been highlighted including glucose transporter 2 (GLUT2), sodium-coupled glucose cotransporters, glucokinase, K_{ATP} channels, Na^+, K^+ ATPase (37; 41-45). Our study highlights that TRPC3 channel constitutes a new player in glucose-sensing. Recent evidences suggested that TRPC channels may be involved the detection of some hormones and nutrients sensing (see for review (11)). For instance, studies showed that the effects of leptin or insulin onto ARC neurons are dependent on TRPC channels (15-17). Nevertheless, the physiologic role of MBH TRPC channels in energy homeostasis has never been investigated *in vivo*. In the present study, we provide physiological evidence that MBH TRPC3 channels contribute to the central control of energy homeostasis and neuronal glucose detection. We demonstrate that TRPC3 channels are expressed in the MBH, a key region of the hypothalamus involved in metabolic sensing. However, none of the commercial or homemade TRPC3 antibodies gave a specific immunohistochemical signal on brain sections (data not shown). Thus, the identity of TRCP3-expressing neurons is yet to be determined. This would particularly be interesting to determine whether TRPC3-expressing neurons are preferentially located in the ARC or VMN within the MBH. Nevertheless, we can speculate that TRPC3-mediated glucose-sensing operate preferentially in ARC GE neurons as work from V. Routh's group showed that VMN GE neurons do not detect directly increased glucose above 5 mM (3).

Our data show that TRPC3 deficiency in the MBH or whole body leads to increases in food intake and body weight thereby suggesting TRPC3 regulates energy balance. Interestingly, whole-body TRPC3 KO mice were also characterized by mild glucose

intolerance and increased basal blood glucose level, a phenotype not observed in $TRPC3^{MBH}$ KO mice. This suggests that TRPC3-expressing MBH neurons could specifically regulate food intake, whereas peripheral or extra-MBH TRPC3-expressing cells could control glucose homeostasis. Consistent with other studies, we found that TRPC3 is expressed in muscle, liver and EWAT. Although the role of TRPC3 in liver and EWAT is unknown (46), studies suggest TRPC3 regulates insulin signaling and glucose uptake in muscle (47; 48)

Surprisingly, we found that the glucose intolerance observed in TRPC3 KO mice is not associated with alteration in insulin sensitivity or secretion. Consistent with this latter parameter, TRPC3 have never been found, to our knowledge, in pancreatic β-cells, which could support an eventual role in insulin secretion. The role of TRPC3 in insulin signaling is however more controversial. In the present study, we show that the decrease in blood glucose level during an ITT or the phosphorylation of AKT in response to insulin in muscles, white adipose depot or liver is not altered in TRPC3 KO mice. These data are not consistent with previous studies showing that TRPC3 channels influence insulin signaling *in vitro* in muscle cells (47; 48). It is possible that the role of TRPC3 channels is not dominant in muscle cells *in vivo* or that TRPC3 deficiency is compensated by other mechanisms. Further studies are required to assess the role of TRPC3 in glucose homeostasis in specific peripheral tissue and organs.

We found that the anorectic effect of glucose as well as the intra-carotid glucose-induced insulin secretion are impaired in TRPC3-deficient mice models. It is noteworthy that this latter result is not consistent with the unaltered insulin secretion observed in TRPC3 KO mice during the OGTT. The intracarotid glucose-induced insulin secretion lasts only 1-3 minutes. Thus, we could hypothesize that affecting only the brain-driven insulin secretion

has only a minimal effect on plasma insulin level when direct pancreatic glucose-induced insulin secretion is triggered during the IPGTT. In addition, oral administration of glucose induces incretins secretion by the gut that potentiate glucose-stimulated insulin secretion and might hide phenotypic differences between WT and KO mice. Nevertheless, these *in vivo* data obtained in TRPC3 KO mice are supported by *in vitro* calcium imaging recordings showing that the glucose response of MBH GE neurons is impaired when TRPC3 expression or activity is altered. Together, these data demonstrate for the first time that TRPC3 channels are a novel actor required for hypothalamic glucose detection and the associated regulation of food intake and insulin secretion.

We show that ROS production is necessary for the response of MBH GE neurons to glucose. Hydrogen peroxide seems the ROS entity of importance based on the impact of the H_2O_2-decomposing enzyme catalase on the glucose response of GE neurons. This is in agreement with previous studies from our group showing that H_2O_2 is produced in the MBH in response to increased brain glucose levels and necessary for glucose modulation of food intake and insulin secretion (7; 8). These results are also consistent with the general role of ROS in the hypothalamic regulation of energy and glucose homeostasis (9; 49).

The fact that ROS production is necessary for the response to glucose of GE neurons suggests that a metabolism-dependent signalling pathway involving multiple cascades is implicated. The necessity of several steps could explain why the latency of GE neurons to respond to glucose is relatively long. However, there is here a discrepancy between the present *in vitro* and *in vivo* data. We found that the intracarotid glucose injection increases insulin secretion within 1-3 minutes whereas GE neurons seem to respond to increased glucose in a longer period of time. Thus, the longer latency in the *in vitro* recordings might reflect the limitation of calcium recordings in dissociated cells in addition to the necessary metabolic steps necessary to increase the electrical activity of GE neurons.

However, a question remains as how ROS modulate TRPC3 activity? Studies show that H_2O_2 increases TRPC3 channel activity (50; 51). It is however unclear if H_2O_2 directly regulates TRPC3 channel activity through the oxidation of cysteine thiol groups or whether H_2O_2 stimulates a redox-sensitive signalling pathway leading to increased TRPC3 activity. It has been suggested that H_2O_2 may indirectly activate TRPC3 channels through the activation of phospholipase C (PLC) (50). This is in agreement with our data showing that OAG, an analogue of DAG generated by PLC, mimics the glucose response in MBH GE neurons.

In view of our data, we cannot rule out that other channel(s) might be involved in glucose responses in GE neurons. Indeed, their response to glucose is not totally blunted in TRPC3-deficient mice. In addition, pharmacological inhibition of TRPC3 activity does not impair the glucose response of all MBH GE neurons tested. Interestingly, the K_{ATP} opener diazoxide did not affect the glucose response of MBH neurons supporting the concept that K_{ATP} channels are not involved in GE neurons response to glucose as previously shown (12). One possible explanation could be that other TRPC isoform(s) contribute to glucose responses in GE neurons. Indeed, the non-selective TRPC channels inhibitor SKF96365 impaired glucose responses in all GE neurons tested suggesting that other TRPC channels may be involved. To support this hypothesis, other TRPC channels have been shown to be redox-sensitive (e.g. TRPC4 and C6 (19)). Interestingly, it was shown that TRPC3 heterodimerizes with TRPC4 channels to form heteromeric redox-sensitive complex in HEK293 and porcine aortic endothelial cells (18). We found that TRPC4 and C6 channels are expressed in the MBH (Supp. Figure 7). Thus, these channels may be potential candidates involved in the glucose response of GE neurons along with the TRPC3 isoform. Of note, we did not observe changes in TRPC4 and C6 expression in the MBH of TRPC3 KO mice suggesting that TRPC3 deficiency is not compensated by other

isoforms (Supp. Figure 7). Further investigations are required to assess whether TRPC4 and/or C6 channel are also involved in glucose sensing.

Another question which still needs to be addressed is whether TRPC3 channels are involved in the detection of other metabolic signals besides glucose. We anticipate that these channels may be part of free fatty acid (FFA)- and/or insulin-sensing mechanisms based on the fact that increased brain FFA or insulin level rises hypothalamic ROS production (52; 53). The role of TRPC3 channels in insulin signalling is reinforced by the fact that insulin has been shown to activate some MBH neurons through TRPC channels (17). The idea that TRPC3 channels might be involved in FFA-sensing is also supported by our results showing that OAG, a DAG analogue, increases the activity of MBH GE neurons and data showing that the incubation of hypothalamic neurons with FFA increases the production of DAG in presence of high glucose level (54). As such, glucose may stimulate the generation of DAG in presence of FFA, which in turn may directly potentiate the response to glucose of MBH GE neurons by activating TRPC3 channels.

In conclusion, the present study demonstrates that TRPC3 channels are required, at the cellular level, to mediate the effect of increased glucose on MBH GE neurons via a mechanism dependent on ROS production. We also show that TRPC3 channels are necessary *in vivo* for the regulation of food intake and insulin secretion in response to increased brain glucose level. Together, our results show that TRPC3 channels are novel players in central glucose sensing and regulation of energy balance.

ACKNOWLEDGEMENTS

Authors are thankful to Dr. Thierry Alquier (University of Montreal, Montreal Diabetes Research Center, Montreal, Canada) for insightful comments and advices on this manuscript. We thank Dr. Richard Palmiter (University of Washington, Seattle, WA, USA) and Dr. Serge Luquet (University Paris Diderot, Paris, France) for providing the plasmid sequence of the AAV-cre/GFP. We are also thankful to A. Lefranc, L. Decocq, E. Lalarme and A. Mathou (CSGA, Dijon, France) for animal care taking. This work was supported by grants from Marie Curie Foundation (CIG NeuROSenS PCIG09-GA-2011-293738, XF), Société Francophone du Diabète (XF). This work was also supported by the following grants: ANR-13-JVS1-0003-01 to AB; ANR-11-BSV1-0007 to CL; SFB 894 by DFG to VF; Z01-ES-101684 to LB. CC was supported by a salary award from Institut National de la Recherche Agronomique (INRA).

Authors declare no conflict of interest.

Dr. X Fioramonti is the guarantor of this work and, as such, had full access to all the data in the study and takes responsibility for the integrity of the data and the accuracy of the data analysis.

Author contributions:

- Research data: XF, CChr, CF, SG, CH, FL, KL, XB, SC, JG, RB, RS, AL, CChe, EN
- Wrote the manuscript: XF, CChr
- Contributed to discussion: XF, CChr, LP, CL, AB
- Review/Edited the manuscript: XF, CChr, LP, AB, ZA, CM, JH, LB, CL, VF.

REFERENCES

1. Schwartz MW, Woods SC, Porte D, Jr., Seeley RJ, Baskin DG: Central nervous system control of food intake. Nature 2000;404:661-671.

2. Fioramonti X, Contie S, Song Z, Routh VH, Lorsignol A, Penicaud L: Characterization of glucosensing neuron subpopulations in the arcuate nucleus: integration in neuropeptide Y and pro-opio melanocortin networks? Diabetes 2007;56:1219-1227

3. Song Z, Levin BE, McArdle JJ, Bakhos N, Routh VH: Convergence of pre- and postsynaptic influences on glucosensing neurons in the ventromedial hypothalamic nucleus. Diabetes 2001;50:2673-2681

4. Oomura Y, Ono T, Ooyama H, Wayner MJ: Glucose and osmosensitive neurones of the rat hypothalamus. Nature 1969;222:282-284.

5. Oomura Y, Ooyama H, Sugimori M, Nakamura T, Yamada Y: Glucose inhibition of the glucose-sensitive neurone in the rat lateral hypothalamus. Nature 1974;247:284-286.

6. Lam TK, Gutierrez-Juarez R, Pocai A, Rossetti L: Regulation of blood glucose by hypothalamic pyruvate metabolism. Science 2005;309:943-947

7. Leloup C, Magnan C, Benani A, Bonnet E, Alquier T, Offer G, Carriere A, Periquet A, Fernandez Y, Ktorza A, Casteilla L, Penicaud L: Mitochondrial reactive oxygen species are required for hypothalamic glucose sensing. Diabetes 2006;55:2084-2090

8. Carneiro L, Allard C, Guissard C, Fioramonti X, Tourrel-Cuzin C, Bailbe D, Barreau C, Offer G, Nedelec E, Salin B, Rigoulet M, Belenguer P, Penicaud L, Leloup C: Importance of mitochondrial dynamin-related protein 1 in hypothalamic glucose sensitivity in rats. Antioxid Redox Signal 2012;17:433-444

9. Andrews ZB, Liu ZW, Walllingford N, Erion DM, Borok E, Friedman JM, Tschop MH, Shanabrough M, Cline G, Shulman GI, Coppola A, Gao XB, Horvath TL, Diano S: UCP2 mediates ghrelin's action on NPY/AgRP neurons by lowering free radicals. Nature 2008;454:846-851

10. Toda C, Kim JD, Impellizzeri D, Cuzzocrea S, Liu ZW, Diano S: UCP2 Regulates Mitochondrial Fission and Ventromedial Nucleus Control of Glucose Responsiveness. Cell 2016;164:872-883

11. Sohn JW: Ion channels in the central regulation of energy and glucose homeostasis. Front Neurosci 2013;7:85

12. Fioramonti X, Lorsignol A, Taupignon A, Penicaud L: A new ATP-sensitive K+ channel-independent mechanism is involved in glucose-excited neurons of mouse arcuate nucleus. Diabetes 2004;53:2767-2775

13. Yang XJ, Kow LM, Funabashi T, Mobbs CV: Hypothalamic glucose sensor: similarities to and differences from pancreatic beta-cell mechanisms. Diabetes 1999;48:1763-1772

14. Nilius B, Voets T: TRP channels: a TR(I)P through a world of multifunctional cation channels. Pflugers Arch 2005;451:1-10

15. Qiu J, Fang Y, Ronnekleiv OK, Kelly MJ: Leptin excites proopiomelanocortin neurons via activation of TRPC channels. The Journal of neuroscience : the official journal of the Society for Neuroscience 2010;30:1560-1565

16. Qiu J, Fang Y, Bosch MA, Ronnekleiv OK, Kelly MJ: Guinea pig kisspeptin neurons are depolarized by leptin via activation of TRPC channels. Endocrinology 2011;152:1503-1514

17. Qiu J, Zhang C, Borgquist A, Nestor CC, Smith AW, Bosch MA, Ku S, Wagner EJ, Ronnekleiv OK, Kelly MJ: Insulin excites anorexigenic proopiomelanocortin neurons via activation of canonical transient receptor potential channels. Cell metabolism 2014;19:682-693

18. Poteser M, Graziani A, Rosker C, Eder P, Derler I, Kahr H, Zhu MX, Romanin C, Groschner K: TRPC3 and TRPC4 associate to form a redox-sensitive cation channel. Evidence for expression of native TRPC3-TRPC4 heteromeric channels in endothelial cells. J Biol Chem 2006;281:13588-13595

19. Song MY, Makino A, Yuan JX: Role of reactive oxygen species and redox in regulating the function of transient receptor potential channels. Antioxid Redox Signal 2011;15:1549-1565

20. Hartmann J, Dragicevic E, Adelsberger H, Henning HA, Sumser M, Abramowitz J, Blum R, Dietrich A, Freichel M, Flockerzi V, Birnbaumer L, Konnerth A: TRPC3 channels are required for synaptic transmission and motor coordination. Neuron 2008;59:392-398

21. Meissner M, Obmann VC, Hoschke M, Link S, Jung M, Held G, Philipp SE, Zimmermann R, Flockerzi V: Lessons of Studying TRP Channels with Antibodies. 2011;

22. Wu Q, Palmiter RD: GABAergic signaling by AgRP neurons prevents anorexia via a melanocortin-independent mechanism. Eur J Pharmacol 2011;660:21-27

23. Fergusson G, Ethier M, Guevremont M, Chretien C, Attane C, Joly E, Fioramonti X, Prentki M, Poitout V, Alquier T: Defective insulin secretory response to intravenous glucose in C57Bl/6J compared to C57Bl/6N mice. Mol Metab 2014;3:848-854

24. Saha JK, Xia J, Grondin JM, Engle SK, Jakubowski JA: Acute hyperglycemia induced by ketamine/xylazine anesthesia in rats: mechanisms and implications for preclinical models. Exp Biol Med (Maywood) 2005;230:777-784

25. Penicaud L, Ferre P, Kande J, Leturque A, Issad T, Girard J: Effect of anesthesia on glucose production and utilization in rats. Am J Physiol 1987;252:E365-369.

26. Dunn-Meynell AA, Routh VH, Kang L, Gaspers L, Levin BE: Glucokinase is the likely mediator of glucosensing in both glucose- excited and glucose-inhibited central neurons. Diabetes 2002;51:2056-2065.

27. Kang L, Routh VH, Kuzhikandathil EV, Gaspers LD, Levin BE: Physiological and molecular characteristics of rat hypothalamic ventromedial nucleus glucosensing neurons. Diabetes 2004;53:549-559

28. Vazirani RP, Fioramonti X, Routh VH: Membrane potential dye imaging of ventromedial hypothalamus neurons from adult mice to study glucose sensing. J Vis Exp 2013;

29. Fioramonti X, Marsollier N, Song Z, Fakira KA, Patel RM, Brown S, Duparc T, Pica-Mendez A, Sanders NM, Knauf C, Valet P, McCrimmon RJ, Beuve A, Magnan C, Routh VH: Ventromedial hypothalamic nitric oxide production is necessary for hypoglycemia detection and counterregulation. Diabetes 2010;59:519-528

30. Routh VH, Hao L, Santiago AM, Sheng Z, Zhou C: Hypothalamic glucose sensing: making ends meet. Front Syst Neurosci 2014;8:236

31. Ciofi P: The arcuate nucleus as a circumventricular organ in the mouse. Neurosci Lett 2011;487:187-190

32. Birnbaumer L: The TRPC class of ion channels: a critical review of their roles in slow, sustained increases in intracellular Ca(2+) concentrations. Annu Rev Pharmacol Toxicol 2009;49:395-426

33. Hartmann J, Konnerth A: TRPC3-dependent synaptic transmission in central mammalian neurons. J Mol Med (Berl) 2015;93:983-989

34. Badin PM, Vila IK, Louche K, Mairal A, Marques MA, Bourlier V, Tavernier G, Langin D, Moro C: High-fat diet-mediated lipotoxicity and insulin resistance is related to impaired lipase expression in mouse skeletal muscle. Endocrinology 2013;154:1444-1453

35. Lanfray D, Arthaud S, Ouellet J, Compere V, Do Rego JL, Leprince J, Lefranc B, Castel H, Bouchard C, Monge-Roffarello B, Richard D, Pelletier G, Vaudry H, Tonon MC, Morin F: Gliotransmission and brain glucose sensing: critical role of endozepines. Diabetes 2013;62:801-810

36. Atef N, Ktorza A, Penicaud L: CNS involvement in the glucose induced increase of islet blood flow in obese Zucker rats. Int J Obes Relat Metab Disord 1995;19:103-107

37. Kang L, Dunn-Meynell AA, Routh VH, Gaspers LD, Nagata Y, Nishimura T, Eiki J, Zhang BB, Levin BE: Glucokinase is a critical regulator of ventromedial hypothalamic neuronal glucosensing. Diabetes 2006;55:412-420

38. Kohno D, Gao HZ, Muroya S, Kikuyama S, Yada T: Ghrelin directly interacts with neuropeptide-Y-containing neurons in the rat arcuate nucleus: Ca2+ signaling via protein kinase A and N-type channel-dependent mechanisms and cross-talk with leptin and orexin. Diabetes 2003;52:948-956

39. Harteneck C, Gollasch M: Pharmacological modulation of diacylglycerol-sensitive TRPC3/6/7 channels. Curr Pharm Biotechnol 2011;12:35-41

40. Hofmann T, Obukhov AG, Schaefer M, Harteneck C, Gudermann T, Schultz G: Direct activation of human TRPC6 and TRPC3 channels by diacylglycerol. Nature 1999;397:259-263

41. Bady I, Marty N, Dallaporta M, Emery M, Gyger J, Tarussio D, Foretz M, Thorens B: Evidence from glut2-null mice that glucose is a critical physiological regulator of feeding. Diabetes 2006;55:988-995

42. Kurita H, Xu KY, Maejima Y, Nakata M, Dezaki K, Santoso P, Yang Y, Arai T, Gantulga D, Muroya S, Lefor AK, Kakei M, Watanabe E, Yada T: Arcuate Na+,K+-ATPase senses systemic energy states and regulates feeding behavior through glucose-inhibited neurons. Am J Physiol Endocrinol Metab 2015;309:E320-333

43. O'Malley D, Reimann F, Simpson AK, Gribble FM: Sodium-coupled glucose cotransporters contribute to hypothalamic glucose sensing. Diabetes 2006;55:3381-3386

44. Parton LE, Ye CP, Coppari R, Enriori PJ, Choi B, Zhang CY, Xu C, Vianna CR, Balthasar N, Lee CE, Elmquist JK, Cowley MA, Lowell BB: Glucose sensing by POMC neurons regulates glucose homeostasis and is impaired in obesity. Nature 2007;449:228-232

45. Leloup C, Orosco M, Serradas P, Nicolaidis S, Penicaud L: Specific inhibition of GLUT2 in arcuate nucleus by antisense oligonucleotides suppresses nervous control of insulin secretion. Brain Res Mol Brain Res 1998;57:275-280.

46. Feng S, Li H, Tai Y, Huang J, Su Y, Abramowitz J, Zhu MX, Birnbaumer L, Wang Y: Canonical transient receptor potential 3 channels regulate mitochondrial calcium uptake. Proc Natl Acad Sci U S A 2013;110:11011-11016

47. Fauconnier J, Lanner JT, Sultan A, Zhang SJ, Katz A, Bruton JD, Westerblad H: Insulin potentiates TRPC3-mediated cation currents in normal but not in insulin-resistant mouse cardiomyocytes. Cardiovasc Res 2007;73:376-385

48. Lanner JT, Bruton JD, Assefaw-Redda Y, Andronache Z, Zhang SJ, Severa D, Zhang ZB, Melzer W, Zhang SL, Katz A, Westerblad H: Knockdown of TRPC3 with siRNA coupled to carbon nanotubes results in decreased insulin-mediated glucose uptake in adult skeletal muscle cells. Faseb J 2009;23:1728-1738

49. Leloup C, Casteilla L, Carriere A, Galinier A, Benani A, Carneiro L, Penicaud L: Balancing mitochondrial redox signaling: a key point in metabolic regulation. Antioxid Redox Signal 2011;14:519-530

50. Groschner K, Rosker C, Lukas M: Role of TRP channels in oxidative stress. Novartis Found Symp 2004;258:222-230; discussion 231-225, 263-226

51. Groschner K, Hingel S, Lintschinger B, Balzer M, Romanin C, Zhu X, Schreibmayer W: Trp proteins form store-operated cation channels in human vascular endothelial cells. FEBS Lett 1998;437:101-106

52. Benani A, Troy S, Carmona MC, Fioramonti X, Lorsignol A, Leloup C, Casteilla L, Penicaud L: Role for mitochondrial reactive oxygen species in brain lipid sensing: redox regulation of food intake. Diabetes 2007;56:152-160

53. Jaillard T, Roger M, Galinier A, Guillou P, Benani A, Leloup C, Casteilla L, Penicaud L, Lorsignol A: Hypothalamic reactive oxygen species are required for insulin-induced food intake inhibition: an NADPH oxidase-dependent mechanism. Diabetes 2009;58:1544-1549

54. Taib B, Bouyakdan K, Hryhorczuk C, Rodaros D, Fulton S, Alquier T: Glucose regulates hypothalamic long-chain fatty acid metabolism via AMP-activated kinase (AMPK) in neurons and astrocytes. The Journal of biological chemistry 2013;288:37216-37229

FIGURES LEGEND

Figure 1: TRPC3 channels are expressed in the MBH. A. TRPC3 mRNA expression obtained by RT-qPCR from cerebellum (Cereb.), MBH, cortex, hippocampus (hippo.), epididymal WAT (EWAT), liver and tibialis anterior (Tib. Ant.) samples (n=6). **B.** Representative Western blot of cerebellum (Cereb.) and MBH against TRPC3.

Figure 2: TRPC3-deficient mice present increased body weight and food intake associated with impaired glucose homeostasis. A. Body weight of TRPC3 WT (n=48) or KO (n=45) mice. **B.** Nocturnal and diurnal food intake of TRPC3 WT (n=11) or KO (n=6) mice. **C.** MBH mRNA expression of NPY, AgRP, POMC and CART from TRPC3 WT (n=9) and KO (n=14) mice. **D.** Fasting blood glucose level of TRPC3 WT (n=37) or KO (n=37) mice. **E.** Blood glucose during an oral glucose tolerance test (OGTT, 2 g/kg, **E *left***) + area under the curve (AUC; **E *insert***) in TRPC3 WT (n=10) or KO (n=8) mice. *: $p<0.05$, ** $p < 0.01$ *vs.* WT unpaired *t*-test; $^{\#}$: $p<0.05$ *vs.* WT, Two-way ANOVA + Bonferroni post-hoc test.

Figure 3: Inhibition of MBH TRPC3 expression increases food intake and body weight gain. A. Representative photo micrograph showing green fluorescent protein (GFP) expression after AAV-cre/GFP virus injection in the MBH of $TRPC3^{lox/lox}$ mice. **B.** MBH and hippocampus (HippoC) TRPC3 mRNA expression in $TRPC3^{lox/lox}$ mice injected in the MBH with an AAV-cre/GFP ($TRPC3^{MBH}$ KO; n=5) or an AAV-GFP ($TRPC3^{MBH}$ WT ; n=6) virus. **C-F.** Body weight gain post-AAV injection (**C**); Average daily food intake measured between week 5 and 6 post AAV injection (**D**); Fasting blood glucose level (**E**) and blood glucose during an IP glucose tolerance test (2 g/kg, **F *left***) + area under the

curve (AUC; **F *insert***) of TRPC3^{MBH} WT (n=19) or KO (n=19) mice. *: p<0.05, *** p < 0.001 *vs.* WT unpaired *t*-test; $^{\#}$: p<0.05 *vs.* WT, Two-way ANOVA + Bonferroni post-hoc test.

Figure 4: MBH TRPC3 channels are required for brain glucose detection. A. Food intake in response to intracerebroventricular (ICV) infusion of glucose or sucrose (lateral ventricule, 0.125 µg in 2 µl infused in 5 min) in 18h fasted-TRPC3 WT (Sucrose: n=6; Glucose: n=5) and TRPC3 KO mice (Sucrose: n=6; Glucose: n=6). **B.** Food intake in response to intraperitoneal infusion of glucose (2 g/kg) or NaCl (0.9 %) in 18h fasted-TRPC3 WT (NaCl: n=7; Glucose: n=8) or TRPC3 KO mice (NaCl: n=6; Glucose: n=7). **C.** Experimental protocol (**C *left***), blood glucose (**C *right top***) and plasma insulin (delta insulin secretion *vs.* t=0; **C *right below***) in response to an intracarotid glucose injection (25 mg/kg) in TRPC3 WT (n=8) and KO (n=13) mice. **D.** Experimental protocol (**D *left***), blood glucose (**D *right above***) or plasma insulin (delta insulin secretion vs. t=0; **D *right below***) in response to an intracarotid glucose injection (9 mg/kg) toward the brain in control rats (n=9) or infused in the MBH with the TRPC3 inhibitor Pyr3 (3 µM; n=8). *: p<0.05, ** p < 0.01 *vs.* WT or Vehicle, Two-way ANOVA + bonferoni post-hoc test. $^{\#}$: p<0.05 *vs*. t0, One-way ANOVA + Bonferroni post-hoc test.

Figure 5: TRPC3-deficient mice present impaired MBH HGE neuron response to increased glucose. A,B. Representative calcium imaging traces of MBH HGE neuron from TRPC3 WT (**A**) or TRPC3 KO mice (**B**). **C,D.** Quantification of glucose response magnitude (AUC, **C**) and latency (**D**) in response to 2.5-10 mM glucose increase in TRPC3 WT (n= 34 HGE neurons/576 total cells) and TRPC3 KO mice (n= 32 HGE neurons/651 totals cells; 4 independent cultures. *: p<0.05, unpaired *t*-test.

Figure 6: TRPC3 channels are required for HGE neurons response to increased glucose. A-C. Representative calcium imaging traces of MBH HGE neuron in response to 2.5-10 mM glucose increase in presence or not of the non-selective TRPC channel inhibitor SKF69365 (5 µM; **A**), the TRPC3 channel inhibitor Pyrazole 3 (Pyr3, 1 µM; **B)** or activated by the TRPC3 activator 2-Acetyl-1-oleoyl-sn-glycerol (OAG, 10 µM; **C**). **D,E.** Quantification of glucose response magnitude (**D**, AUC) and latency (**E**) of the second response to 10 mM increased glucose level in presence of solvent (Glucose alone) or TRPC channels modulators of cells presenting a residual response. **: p<0.01, ***: p<0.001 *vs.* 1st glucose response, paired *t*-test; ns: p>0.05; $^{###}$: p<0,001 *vs.* Glucose, one-way ANOVA + Bonferroni post-hoc test.

Figure 7: **ROS are involved in HGE neuron response to increased glucose. A, B.** Representative calcium imaging traces of MHB HGE neuron in response to 2.5-10 mM glucose increase in presence or not a cocktail of non-selective Trolox/GSH antioxidants (Trolox 0.2 mM + Glutathion (GSH) 0.1 mM, **A**) or the selective H_2O_2-removing enzyme catalase (4000 U/ml, **B**). **C,D.** Quantification of glucose response magnitude (**C**) and latency (**D**) of the second response to 10 mM increased glucose level in presence of solvent (Glucose alone) or antioxidants of cells presenting a residual response. **: p<0.01, ***: p<0.001 *vs.* 1st glucose response, paired *t*-test; ns: p>0.05 *vs.* Glucose, one-way ANOVA + Bonferroni post-hoc test.

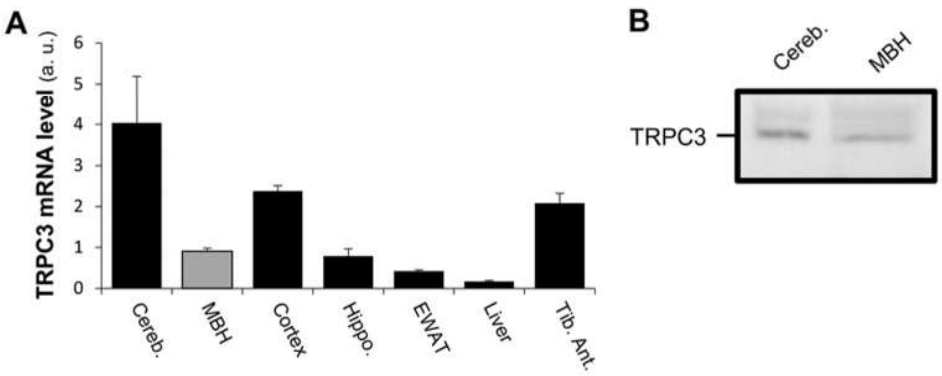

Figure 1: TRPC3 channels are expressed in the MBH. A. TRPC3 mRNA expression obtained by RT-qPCR from cerebellum (Cereb.), MBH, cortex, hippocampus (hippo.), epididymal WAT (EWAT), liver and tibialis anterior (Tib. Ant.) samples (n=6). B. Representative Western blot of cerebellum (Cereb.) and MBH against TRPC3.

74x30mm (300 x 300 DPI)

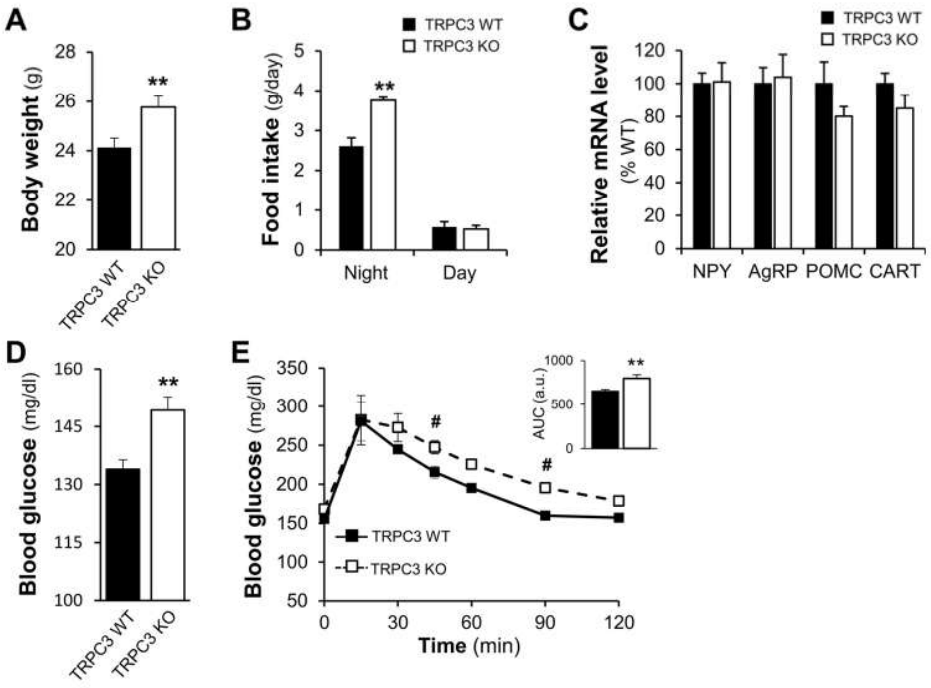

Figure 2: TRPC3-deficient mice present increased body weight and food intake associated with impaired glucose homeostasis. A. Body weight of TRPC3 WT (n=48) or KO (n=45) mice. B. Nocturnal and diurnal food intake of TRPC3 WT (n=11) or KO (n=6) mice. C. MBH mRNA expression of NPY, AgRP, POMC and CART from TRPC3 WT (n=9) and KO (n=14) mice. D. Fasting blood glucose level of TRPC3 WT (n=37) or KO (n=37) mice. E. Blood glucose during an oral glucose tolerance test (OGTT, 2 g/kg, E left) + area under the curve (AUC; E insert) in TRPC3 WT (n=10) or KO (n=8) mice. *: $p<0.05$, ** $p < 0.01$ vs. WT unpaired t-test; #: $p<0.05$ vs. WT, Two-way ANOVA + Bonferroni post-hoc test.

133x99mm (300 x 300 DPI)

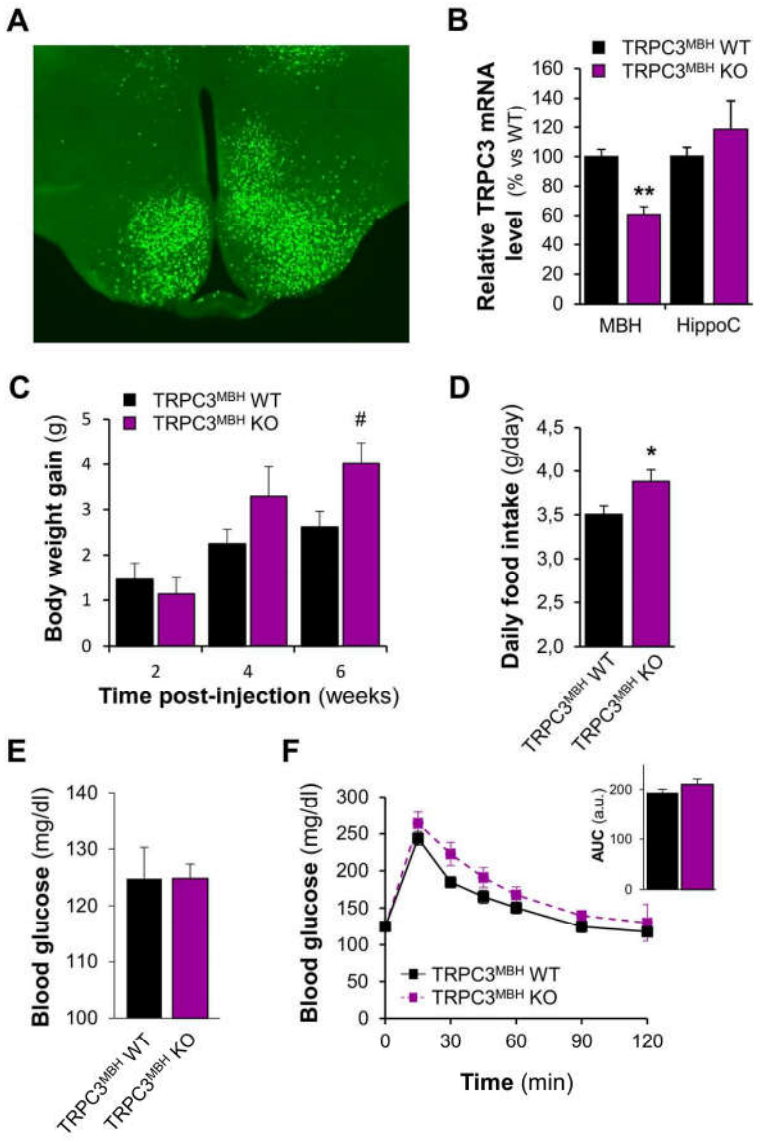

Figure 3: Inhibition of MBH TRPC3 expression increases food intake and body weight gain. A. Representative photo micrograph showing green fluorescent protein (GFP) expression after AAV-cre/GFP virus injection in the MBH of TRPC3lox/lox mice. B. MBH and hippocampus (HippoC) TRPC3 mRNA expression in TRPC3lox/lox mice injected in the MBH with an AAV-cre/GFP (TRPC3MBH KO; n=5) or an AAV-GFP (TRPC3MBH WT ; n=6) virus. C-F. Body weight gain post-AAV injection (C); Average daily food intake measured between week 5 and 6 post AAV injection (D); Fasting blood glucose level (E) and blood glucose during an IP glucose tolerance test (2 g/kg, F left) + area under the curve (AUC; F insert) of TRPC3MBH WT (n=19) or KO (n=19) mice. *: $p<0.05$, *** $p < 0.001$ vs. WT unpaired t-test; #: $p<0.05$ vs. WT, Two-way ANOVA + Bonferroni post-hoc test.

267x397mm (300 x 300 DPI)

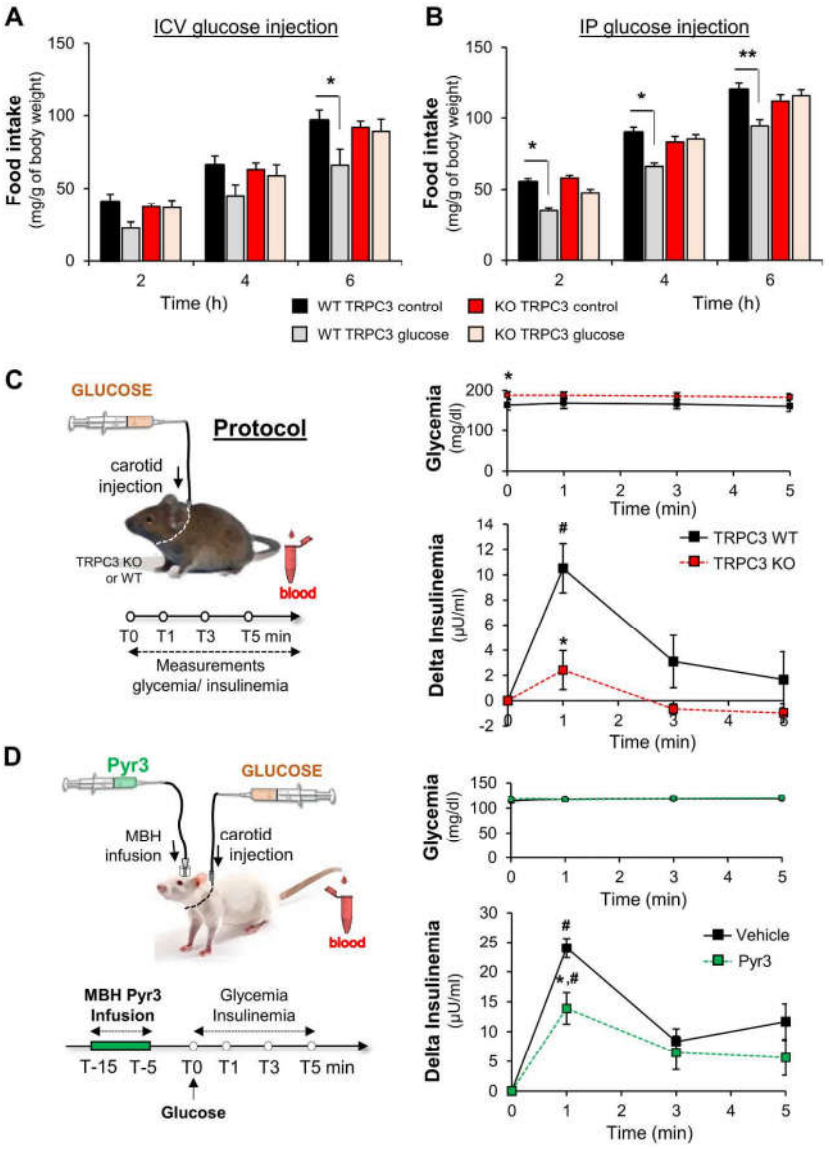

Figure 4: MBH TRPC3 channels are required for brain glucose detection. A. Food intake in response to intracerebroventricular (ICV) infusion of glucose or sucrose (lateral ventricule, 0.125 µg in 2 µl infused in 5 min) in 18h fasted/TRPC3 WT (Sucrose: n=6; Glucose: n=5) and TRPC3 KO mice (Sucrose: n=6; Glucose: n=6). B. Food intake in response to intraperitoneal infusion of glucose (2 g/kg) or NaCl (0.9 %) in 18h fasted/TRPC3 WT (NaCl: n=7; Glucose: n=8) or TRPC3 KO mice (NaCl: n=6; Glucose: n=7). C. Experimental protocol (C left), blood glucose (C right top) and plasma insulin (delta insulin secretion vs. t=0; C right below) in response to an intracarotid glucose injection (25 mg/kg) in TRPC3 WT (n=8) and KO (n=13) mice. D. Experimental protocol (D left), blood glucose (D right above) or plasma insulin (delta insulin secretion vs. t=0; D right below) in response to an intracarotid glucose injection (9 mg/kg) toward the brain in control rats (n=9) or infused in the MBH with the TRPC3 inhibitor Pyr3 (3 µM; n=8). *: p<0.05, ** p < 0.01 vs. WT or Vehicle, Two/way ANOVA + bonferoni post/hoc test. #: p<0.05 vs. t0, One/way ANOVA + Bonferroni post/hoc test.

235x306mm (300 x 300 DPI)

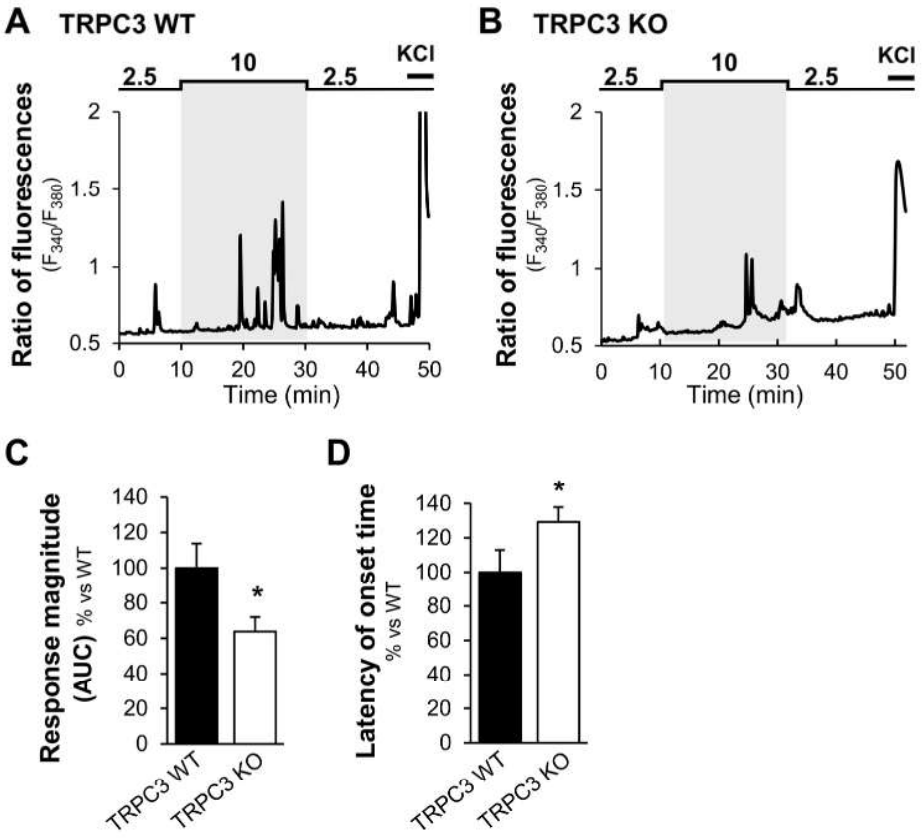

Figure 5: TRPC3-deficient mice present impaired MBH HGE neuron response to increased glucose. A,B. Representative calcium imaging traces of MBH HGE neuron from TRPC3 WT (A) or TRPC3 KO mice (B). C,D. Quantification of glucose response magnitude (AUC, C) and latency (D) in response to 2.5-10 mM glucose increase in TRPC3 WT (n= 34 HGE neurons/576 total cells) and TRPC3 KO mice (n= 32 HGE neurons/651 totals cells; 4 independent cultures. *: $p<0.05$, unpaired t-test.

165x151mm (300 x 300 DPI)

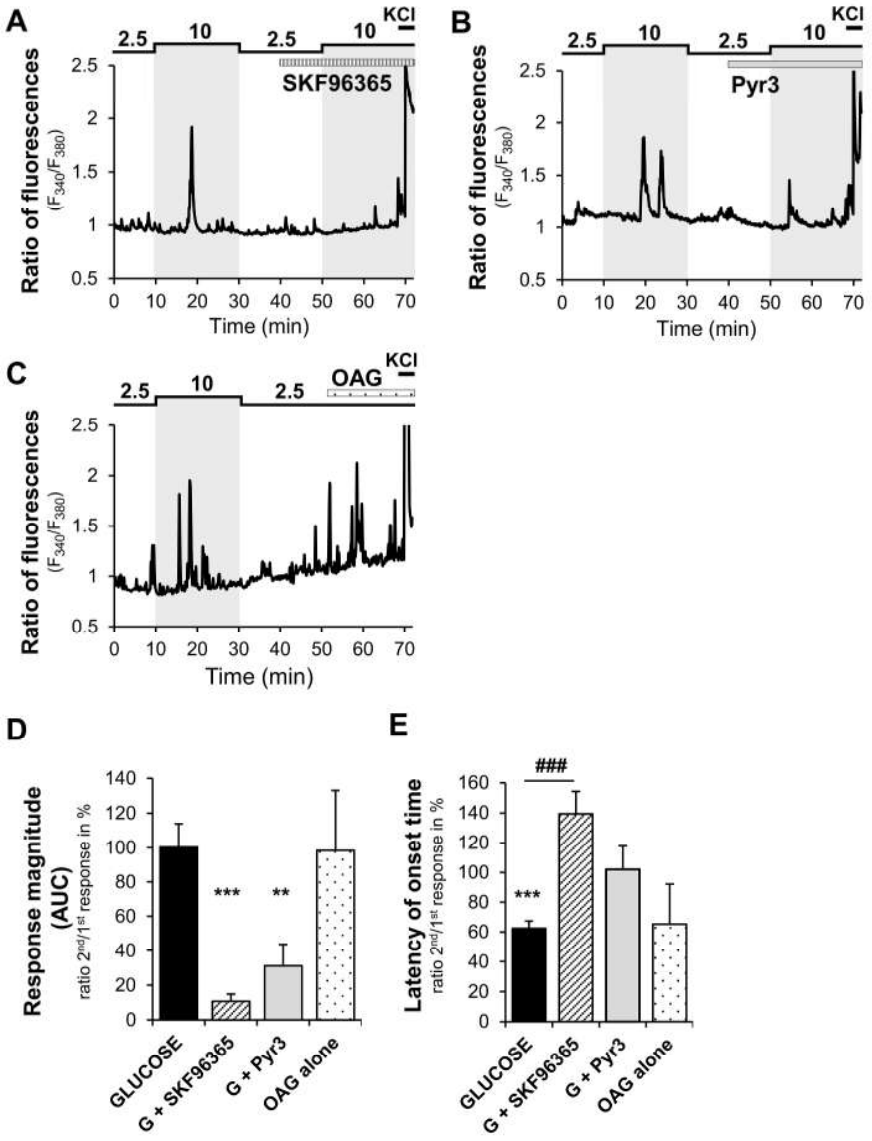

Figure 6: TRPC3 channels are required for HGE neurons response to increased glucose. A-C. Representative calcium imaging traces of MBH HGE neuron in response to 2.5-10 mM glucose increase in presence or not of the non-selective TRPC channel inhibitor SKF69365 (5 µM; A), the TRPC3 channel inhibitor Pyrazole 3 (Pyr3, 1 µM; B) or activated by the TRPC3 activator 2-Acetyl-1-oleoyl-sn-glycerol (OAG, 10 µM; C). D,E. Quantification of glucose response magnitude (D, AUC) and latency (E) of the second response to 10 mM increased glucose level in presence of solvent (Glucose alone) or TRPC channels modulators of cells presenting a residual response. **: $p<0.01$, ***: $p<0.001$ vs. 1st glucose response, paired t-test; ns: $p>0.05$; ###: $p<0,001$ vs. Glucose, one-way ANOVA + Bonferroni post-hoc test.

234x305mm (300 x 300 DPI)

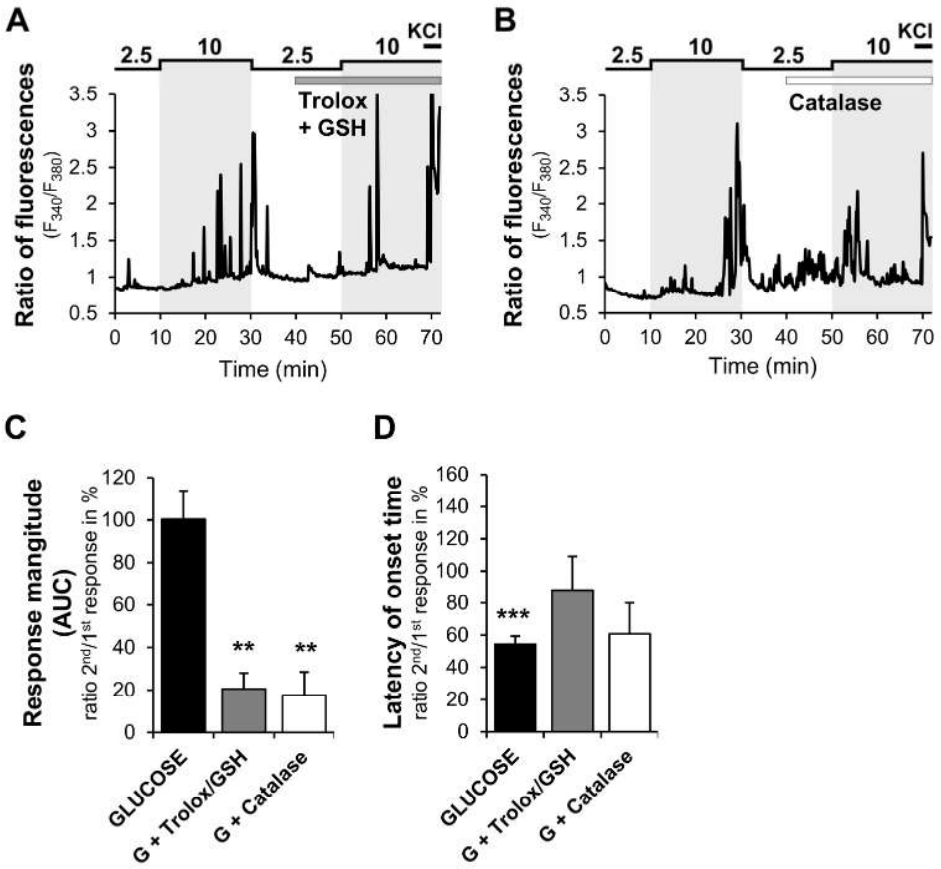

Figure 7: ROS are involved in HGE neuron response to increased glucose. A, B. Representative calcium imaging traces of MHB HGE neuron in response to 2.5-10 mM glucose increase in presence or not a cocktail of non-selective Trolox/GSH antioxidants (Trolox 0.2 mM + Glutathion (GSH) 0.1 mM, A) or the selective H2O2-removing enzyme catalase (4000 U/ml, B). C,D. Quantification of glucose response magnitude (C) and latency (D) of the second response to 10 mM increased glucose level in presence of solvent (Glucose alone) or antioxidants of cells presenting a residual response. **: $p<0.01$, ***: $p<0.001$ vs. 1st glucose response, paired t-test; ns: $p>0.05$ vs. Glucose, one-way ANOVA + Bonferroni post-hoc test.

168x158mm (300 x 300 DPI)

PCR assay	Gene	Primers sequence or reference (Applied Biosystem)
SYBR green assay	NPY	NPY-F: CCGCCACGATGCTAGGTAAC
		NPY-R: CAGCCAGAATGCCCAAACAC
	AgRP	AgRP-F: CAGCCAGAATGCCCAAACAC
		AgRP-R: GACTCGTGCAGCCTTACACAG
	POMC	POMC-F: GCGACGGAAGAGAAAAGAGGT
		POMC-R: ATTGGAGGGACCCCTGTCG
	CART	CART-F: CACGAGAAGGAGCTGCCAAG
		CART-R: GACTCGTGCAGCCTTACACAG
	UBC	UBC-F: CCCACACAAAGCCCCTCAAT
		UBC-R: AAGATCTGCATCGTCTCTCTCAC
TaqMan assay	TRPC3	Mm00444690_m1
	TRPC4	Rn00584835_m1
	TRPC6	Rn00677559_m1
	36B4	Rn03302271_gH
	TBP	Mm00446973_m1
	UBC	Mm01198158_m1

Supp. Table 1: Primers sequence or reference used for SYBR green or Taqman assays.

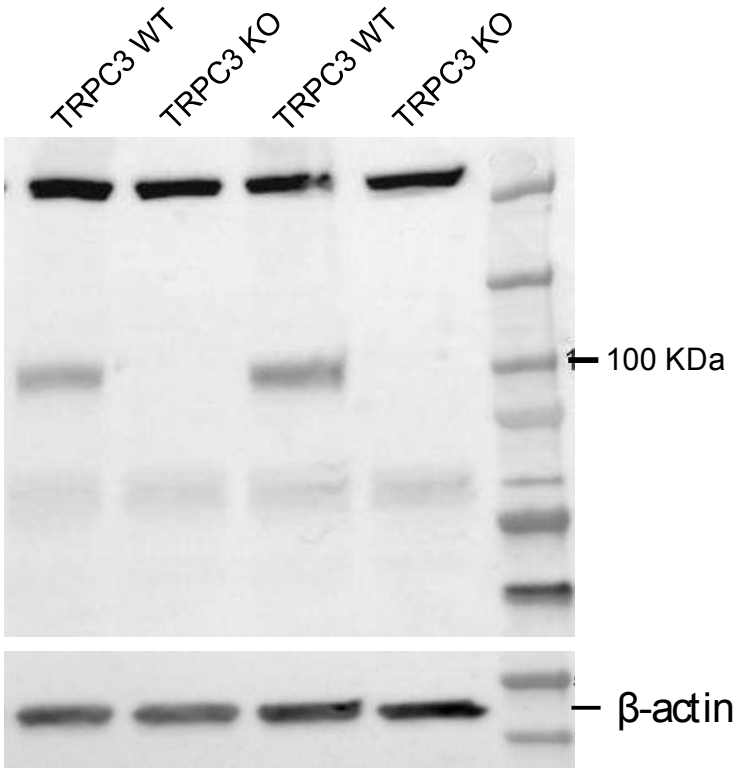

Supp. Figure 1: Validation of the TRPC3 antibody. Representative western blot of cerebellum samples from TRPC3 WT and KO mice against TRPC3 (top) or β-actin proteins (bottom).

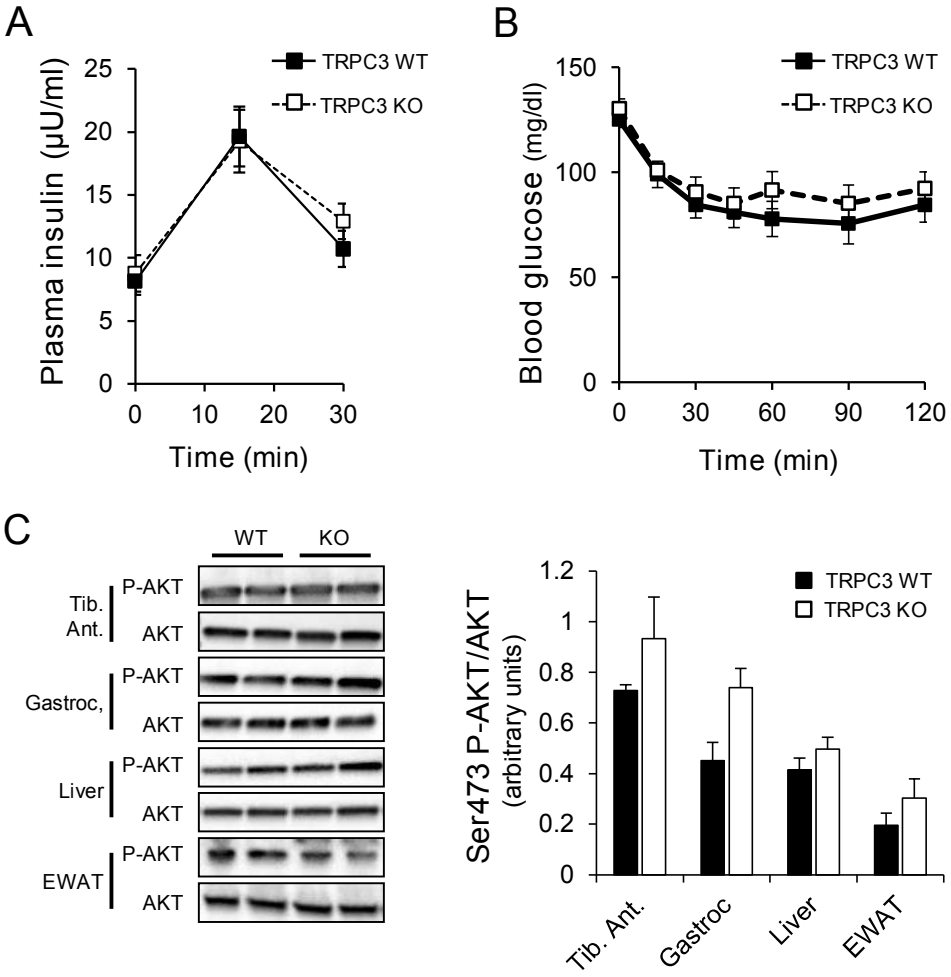

Supp. Figure 2: Insulin secretion and sensitivity are not altered in TRPC3 KO mice. A. Glucose-stimulated plasma insulin levels during the OGTT in TRPC3 WT (n=10) or KO (n=8) mice. B. Blood glucose during an insulin tolerance test (ITT; 0.3 U/kg) in TRPC3 WT (n=12) or TRPC3 KO (n=10) mice. C. Representative blots of Ser473 pAkt and total Akt (C left) and quantitative bar graphs of Ser473-Akt phosphorylation (C right) in tibialis anterior (Tib. Ant.) and gastrocnemius (Gastroc) muscles, liver and epididymal white adipose tissue (EWAT) in TRPC3 WT (n=6) and KO (n=8) mice fasted for 5 hours 10 minutes after insulin injection (IP, 10 U/kg). Procedure for P-Akt western blotting was performed as previously described (ref. 28).

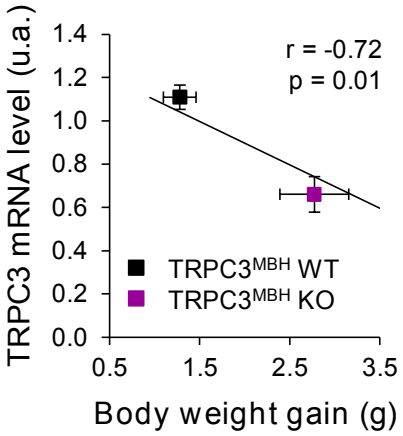

Supp. Figure 3: Decreased MBH TRPC3 expression is correlated with increased body weight gain. Strength of association by the Pearson correlation test between MBH TRPC3 expression and body weight gain of $TRPC3^{lox/lox}$ mice injected in the MBH with an AAV-cre/GFP ($TRPC3^{MBH}$ KO; n=5) or an AAV-GFP ($TRPC3^{MBH}$ WT ; n=6) virus.

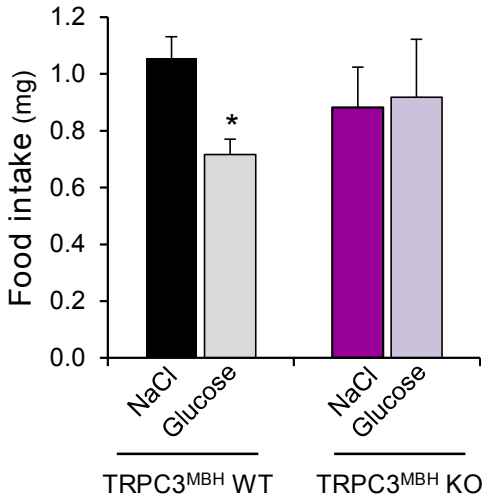

Supp. Figure 4: Inhibition of MBH TRPC3 expression impairs IP glucose-induced decreased food intake. Food intake 2 hours after intraperitoneal injection of glucose (2 g/kg) or NaCl (0.9 %) in 18h fasted-TRPC3^{MBH} WT (NaCl: n=7; Glucose: n=7) or TRPC3^{MBH} KO mice (NaCl: n=5; Glucose: n=7), 6 weeks post-AAV-injection.

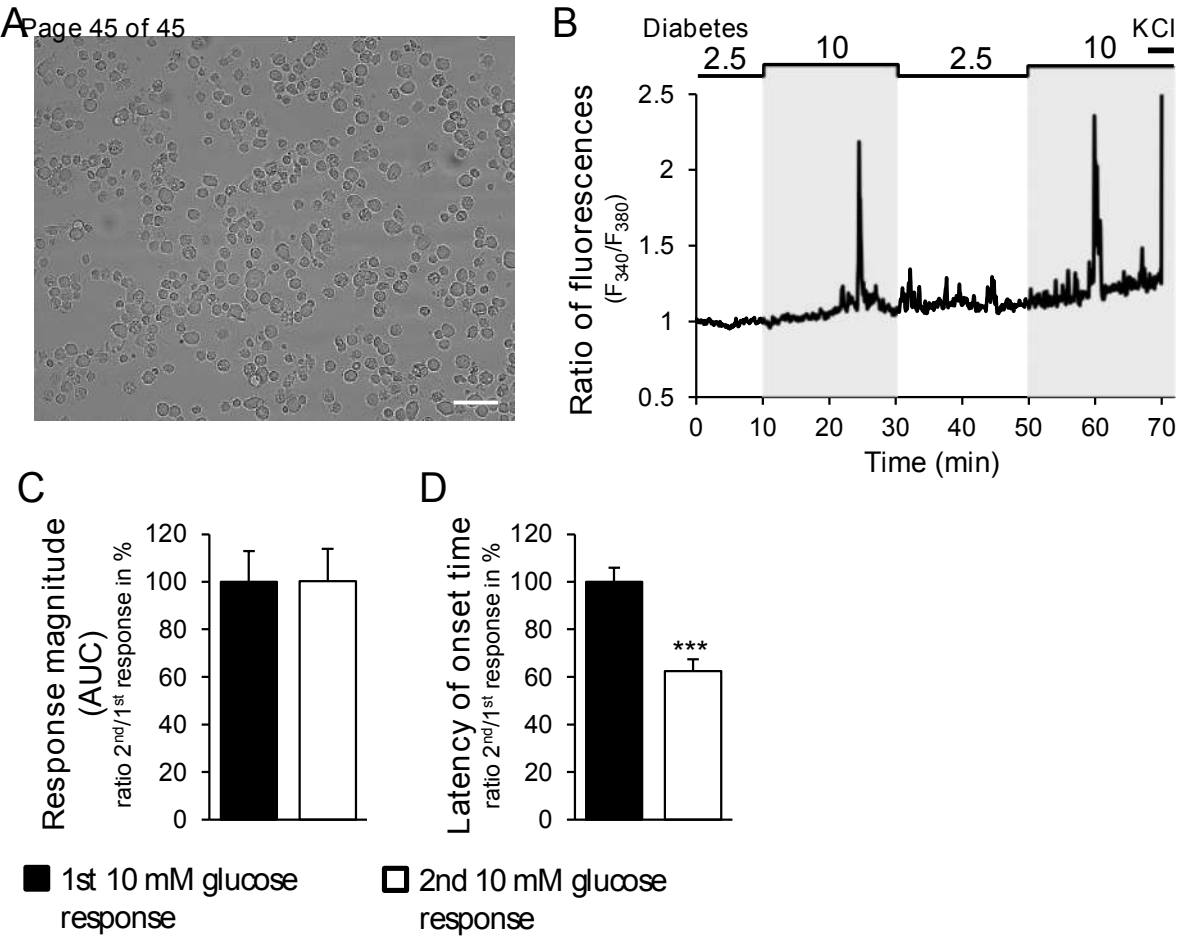

Supp. Figure 5: Characterization of MBH HGE neuron in response to increased glucose level. A- Representative bright-field image of cultured dissociated MBH neurons (x20 objective, scale bar = 40 µm). B- Representative calcium imaging trace of HGE neuron in response to 2 consecutives increased glucose level from 2.5 to 10 mM. Quantification of the magnitude (AUC, C) and latency (D) of the 1st and 2nd glucose response (B; n=71 HGE neurons/953 total cells, 16 independent cultures).***: $p<0.05$ vs. 1st glucose response, paired t-test.

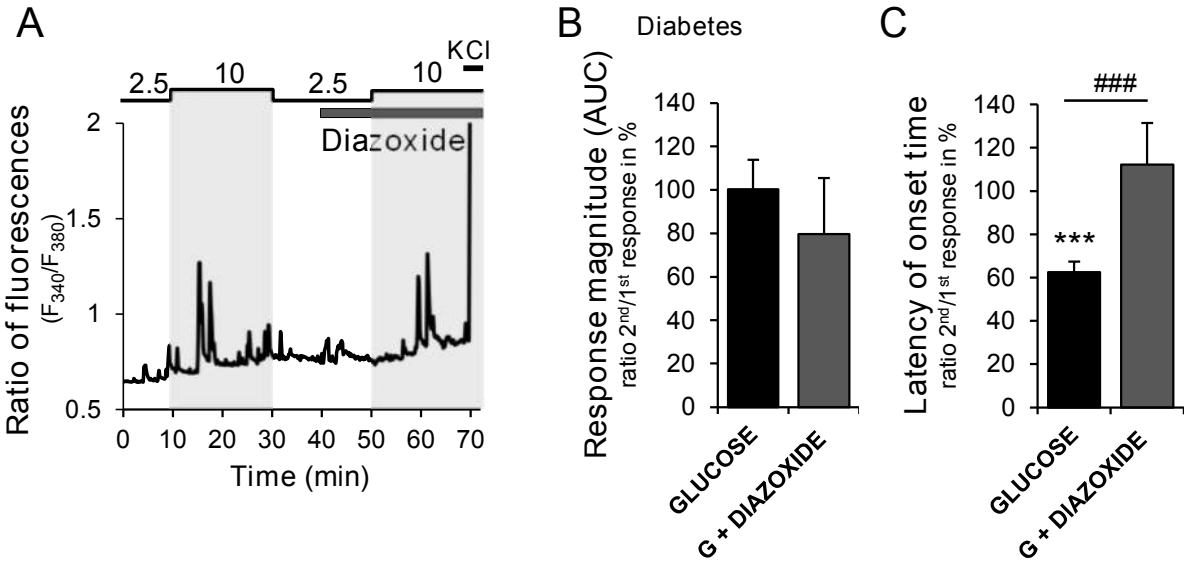

Supp. Figure 6: K_{ATP} channels are not involved in GE neuron response to increased glucose. A. Representative calcium imaging traces of MHB HGE neuron in response to 2.5-10 mM glucose increase in presence or not of potassium channel activator Diazoxide (250µM). B,C. Quantification of glucose response magnitude (B) and latency (C) of the second response to 10 mM increased glucose level in presence of solvent (Glucose alone) or Diazoxide. ***: $p<0.001$ vs. 1st glucose response, paired t-test; ns: $p>0.05$, ###: $p<0,001$ vs. Glucose, unpaired t-test.

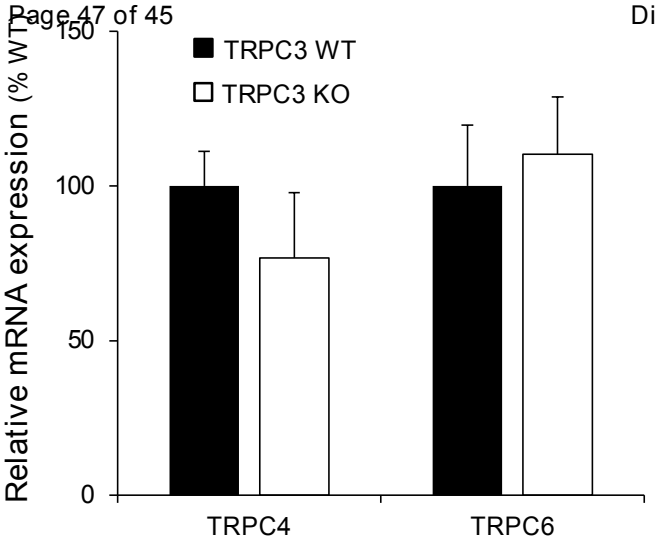

Supp. Figure 7: TRPC3 deficient mice do not have altered MBH TRPC4 and C6 expression. MBH TRPC4 and TRPC6 mRNA expression in TRPC3 WT (n=10) and KO (n=14) mice.